Supplement of

Iodine oxoacids and their roles in sub-3 nanometer particle growth in polluted urban environments

Ying Zhang[1,2,3,★], Duzitian Li[2,3,★], Xu-Cheng He[4,5], Wei Nie[2,3], Chenjuan Deng[6], Runlong Cai[4], Yuliang Liu[2,3], Yishuo Guo[1], Chong Liu[2,3], Yiran Li[6], Liangduo Chen[2,3], Yuanyuan Li[2,3], Chenjie Hua[1], Tingyu Liu[1], Zongcheng Wang[1], Lei Wang[2,3], Tuukka Petäjä[4], Federico Bianchi[4], Ximeng Qi[2,3], Xuguang Chi[2,3], Pauli Paasonen[4], Yongchun Liu[1], Chao Yan[2,3], Jingkun Jiang[6], Aijun Ding[2,3], Markku Kulmala[1,2,3,4]

Correspondence to: Xu-Cheng He (xucheng.he@helsinki.fi) and Wei Nie (niewei@nju.edu.cn)

Text

S1. Field measurements of sulphur dioxide (SO_2) at two sites

SO_2 is measured continuously at the SORPES station using a Thermo TEI 43i. At BUCT/AHL station, SO_2 is measured with the same analyser. Due to an instrument malfunction, SO_2 concentration is discarded in October and November, 2020 at the BUCT/AHL station. The long-term time traces of daytime (08:00~16:00 LT) mean SO_2 and its seasonal and monthly variations at both sites are depicted in Fig. S1. SO_2 is primarily emitted through coal combustion in heating seasons in Beijing. The official onset of the heating period in Beijing is 15th November and the heating ends on 15th March the following year. The SO_2 at BUCT/AHL site is strongly enhanced by the release of SO_2 in heating seasons (grey shade area). It is worth noting that the measured concentrations of SO_2 at the BUCT/AHL station is higher than that of the SORPES station in winter (January and February), which could partially explain the higher concentration of H_2SO_4 measured in Beijing.

S2. Classification of growth time span at SORPES

A Neutral cluster and Air Ion Spectrometer (NAIS, Airel Ltd., Estonia) (Manninen et al., 2016) was deployed to detect the particle number size distribution (PNSD) in the early stages of NPF at the SORPES station. The negatively charged particles in the size range of around 0.8 nm to 42 nm were measured to

study the growth of newly formed particles. However, the limited charges are likely to be captured by larger particles in polluted urban environments which leaves it difficult for us to track the growth trajectory of sub-3 nm particles in NPF events in the SORPES station.

To compare the contribution of gaseous HIO_3 in the subsequent growth of newly formed particles in NPF events at the SORPES station, we further developed a new method by considering gaseous H_2SO_4 as the governing GR contributor as mentioned in 2.2.2. To get the average acid concentration, the general NPF timespan needs to be determined. Though the growth trajectories of smaller particles are vague in this study, the 50% appearance time at approximately 7 nm, where the PNSD shows a sharp increase, can be identified (Kulmala et al., 2012). The 50% appearance time at 7 nm is therefore regarded as the end time for the particle formation as this study focuses on the sub-7 nm particle growth processes. We further find the start time of NPF events by extrapolating different hours backward in time. To better reflect the uncertainty induced by different timespans, we further show the statistical results for each timespan in Fig. S8. As the acid concentration time resolution is 30 min, different time spans (0.5, 1, 1.5 and 2 hours) are investigated to determine which one is the most suitable for all individual NPF cases. Figure S8(a) shows the scatterplot of iodic acid contribution to growth versus that of sulfuric acid for sub-3 nm particles. The GR contribution of IA accounts for no less than 1% and no larger than 20% compared to SA. It should be noted that the slope of the fitted line remains nearly unchanged and the ratio varies inconspicuously as the timespan increases from 0.5 h to 2 h. Therefore, different timespan determination will not induce significant uncertainty in the calculated GR contribution. Figure S8(b) shows the boxplot of the ratio of iodic acid contribution to that of sulfuric acid for sub-3 nm particles using different timespans. It can be seen that with the increasement of growth timespan from 0.5 h to 2 h, the contribution ratio rise insignificantly. We therefore choose the 2 hours timespan in this study as the sub-7 nm growth in Beijing is regularly at a few nanometers per hour (Table S2 – S9) and a 2-hours window should generally contain the period when the particles grow from sub-3 nm to 7 nm. The statistical result for all NPF events at the SORPES station is depicted in Fig. S8(c).

S3. The sensitivity of survival probability

The non-linear relationship between survival probability and growth rate and the coagulation sink given by Eq. (8) suggests that a small perturbation of growth rate could lead to a significant shift of particle

survival probability. As depicted in Fig. 5, the theoretical SP for both sub-3 nm and 3-7 nm particles can vary significantly with different coagulation sink and growth rates. At a fixed coagulation sink, the difference in GR of a factor of 10 contributes to a difference in SP of a factor of around 1000, which reflects that the SP of particles are extremely sensitive to the change of GR.

To further illustrate this sensitivity of survival probability to growth rate change, we quantify the sensitivity of SP to particle GR difference (ΔGR) in Fig. S9. The sensitivity of SP in this study is quantified using the amplification of SP induced by GR difference (X-axis) and is calculated according to

$$\text{SP amplification} = \frac{\text{SP}(\text{GR}_0 + \Delta\text{GR})}{\text{SP}(\text{GR}_0)} \quad (14)$$

where GR_0 refers to the initial growth rate of particles, and ΔGR is the difference in GR. SP(GR_0) and $\text{SP}(\text{GR}_0 + \Delta\text{GR})$ are the theoretical SP calculated using Eq. (8). The results of SP amplification with different GR_0 (1.0 and 1.5 nm h^{-1}) are shown in Fig. S9(b) and S9(c), respectively. The amplification of SP caused by additional GR enhancement is both subject to the particle diameter, d_p and GR_0. Fig. S9(b) shows that for particles growing initially at the rate of 1.0 nm h^{-1}, the smaller the particles are and the larger the GR increases, the more significant the amplification of SP. Fig. S9(c) depicts that particle SP will be amplified less significantly if particles grow at a higher initial rate (1.5 nm h^{-1}). To better bridge the gap between measurement results and theoretical calculation, Fig. S9(a) shows the frequency distribution of iodic acid GR contribution at the SORPES station as a case study. At the SORPES station, sulphuric acid dominates the initial growth of sub-3 nm particles. Therefore, GR contribution of IA can be taken into consideration as additional GR increment (ΔGR). For new particles growing at the rate of around 1 nm h^{-1} at the SORPES station, iodic acid as an additional GR contributor could regularly amplify the particles SP to 2 orders of magnitude higher. Fig. S8(c) also illustrate that iodic acid GR contribution will significantly enhance the SP of sub-3 nm particles accounting for no more than 20% of sulphuric acid GR contribution. This case study shows that the high sensitivity of particles SP to GR difference makes it rather difficult to characterize a NPF event, especially in urban environments with various GR contributors.

S4. Cluster analysis of backward trajectories

To analyse the air masses reaching the AHL/BUCT site, we conducted cluster analysis of backward trajectory using the TrajStat model, a plug-in of MeteoInfo software (Wang, 2014). The calculation of trajectories was based on the Hybrid Single-Particle Lagrangian Integrated Trajectory (HYSPLIT) model (Cohen et al., 2015). As depicted in Fig. S3, the 3-day backward trajectories at 500 m above the ground level of the AHL/BUCT station (39˚56′N, 116˚17′E) are clustered by examining the total spatial variance (TSV).

Figures

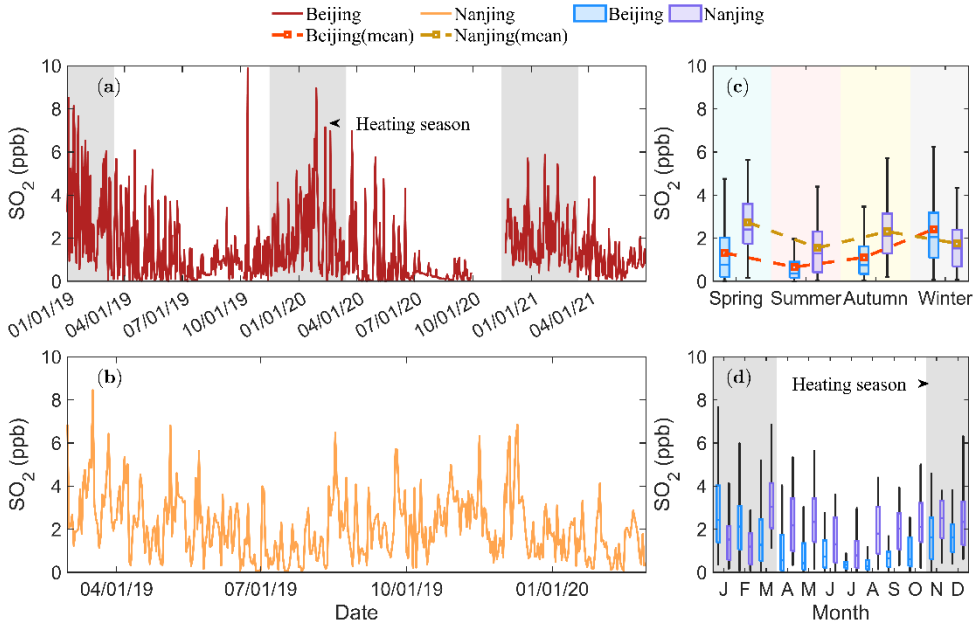

Figure S1. Measurements of SO_2 at two sites. The time traces of measured mean values of daytime (08:00~16:00 LT) SO_2 are shown in (a) and (b) for the BUCT/AHL station and the SORPES station, respectively. Seasonal (c) and monthly (d) variations at both sites are computed by the daytime mean values as well. The heating period in Beijing are depicted by the grey shaded areas in (a) and (c).

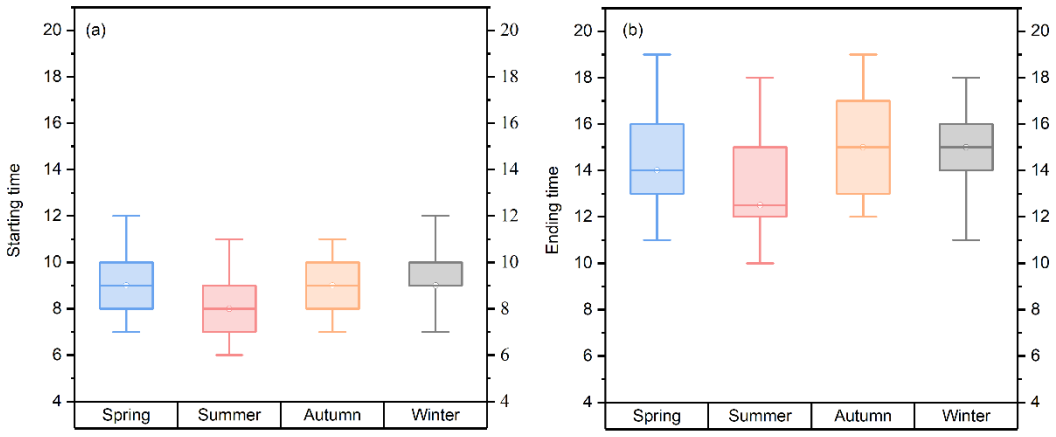

Figure S2. Starting time (a) and ending time (b) of NPF events in Beijing four seasons.

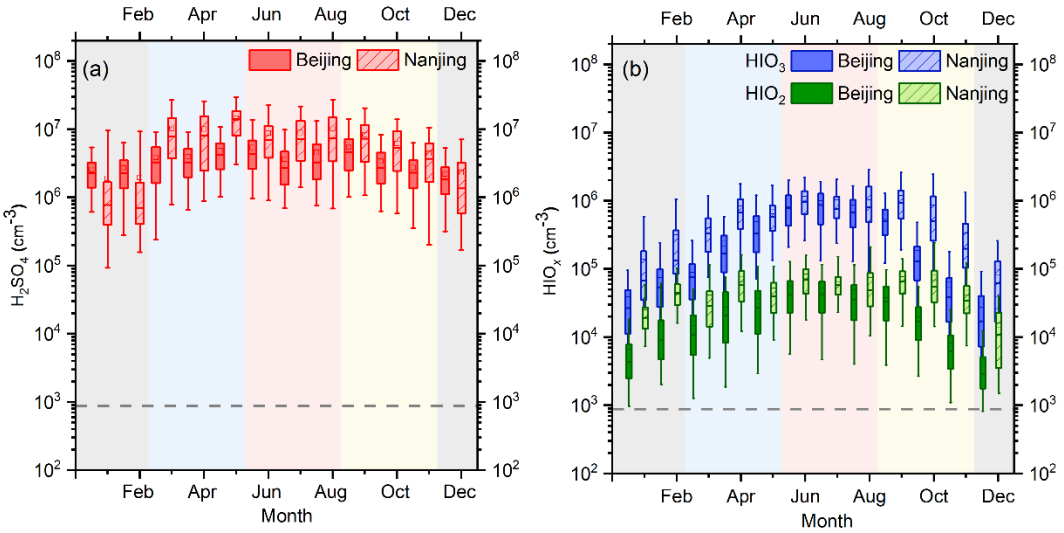

Figure S3. Monthly variation of sulfuric acid and iodine oxoacid concentrations in Beijing and Nanjing.

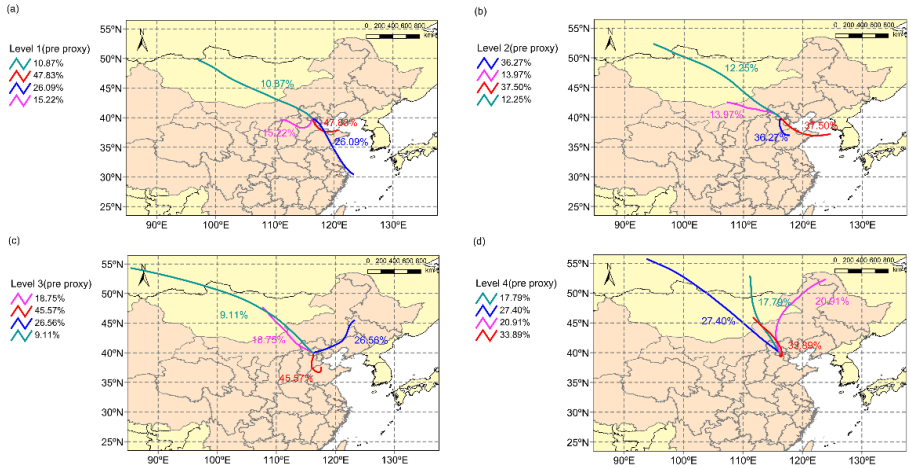

Figure S4. The cluster analysis in different HIO_3 precursors intensities. The four levels of the proxy concentration of HIO_3 precursors are in the 75% - 100%, 50%-75%, 25%-50%, 0-25% percentiles from the first to the fourth levels, respectively.

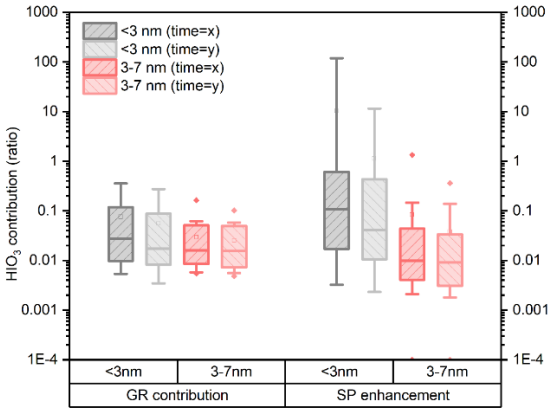

Figure S5. The contributions of HIO_3 to growth rate and survival probability of particles within sub-3nm and 3-7 nm in NPF events using the 50% appearance time method.

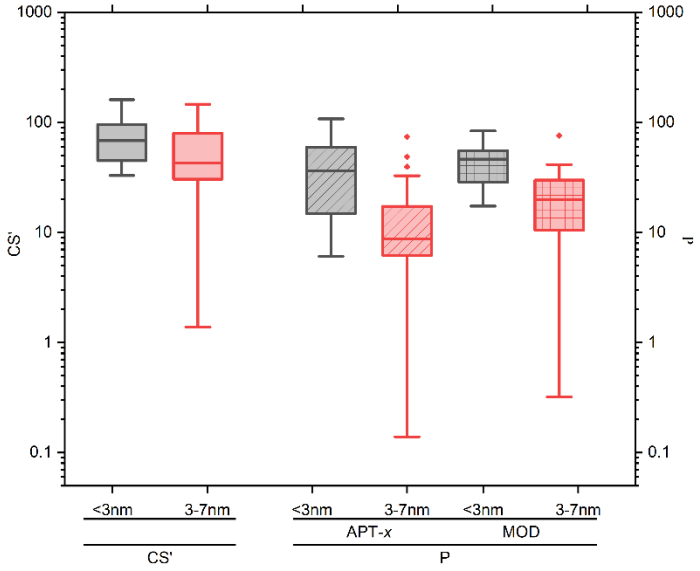

Figure S6. The dimensionless CS' and P in the growth periods within sub-3 nm and 3-7 nm. Here, CS' are calculated from CS (unit: s^{-1}) divided by 10^{-4} s^{-1} and the P is the ratio of CS' and GR' (GR/(1 nm h^{-1})). Both of them are calculated based on Kulmala et al. (2017).

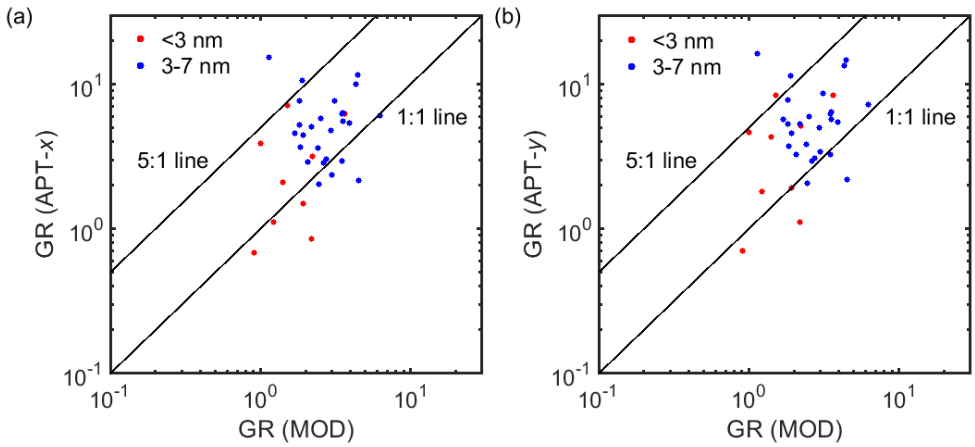

Figure S7. The measured GR comparison between two different methods. (a) Comparison between APT-*x* and MOD and (b) comparison between APT-*y* and MOD.

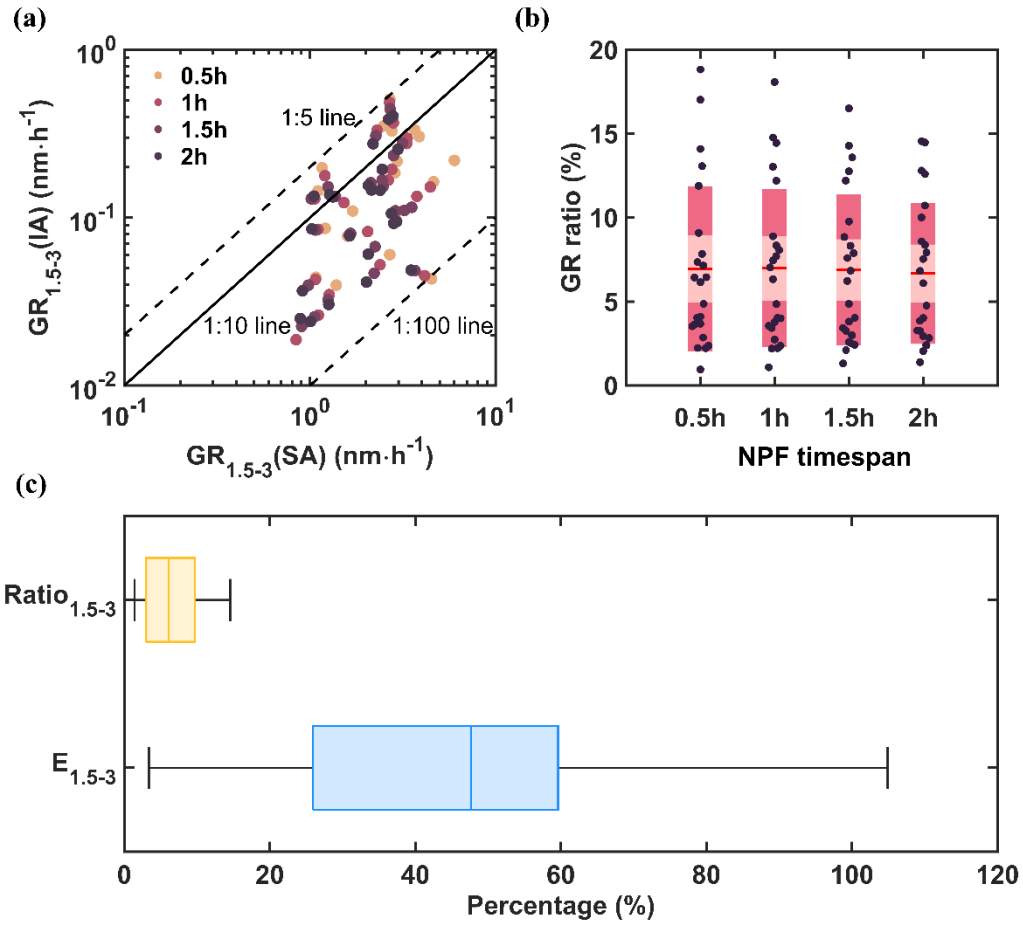

Figure S8: Determination of NPF timespan and the statistical result showing the GR contribution and hence SP enhancement in percentage considering HIO_3 as additional GR contributor. The scatterplot of GR contribution of HIO_3 to particles growing from 1.5 nm to 3nm versus that of H_2SO_4 coloured by different NPF timespans is presented in (a). Boxplots of the calculated ratio are shown in (b), in which the red solid line in the middle is the mean value of contribution ratio in each timespan bin. Calculted GR ratio for each NPF events are points drawn along Y axis. Points are laid over a 1.96 SEM (95% confidence interval) area shaded in rosy brown and one standard deviation area shaded in dark red. The boxplots for GR contribution ratio and SP enhancements at the SORPES station are depicted in (c).

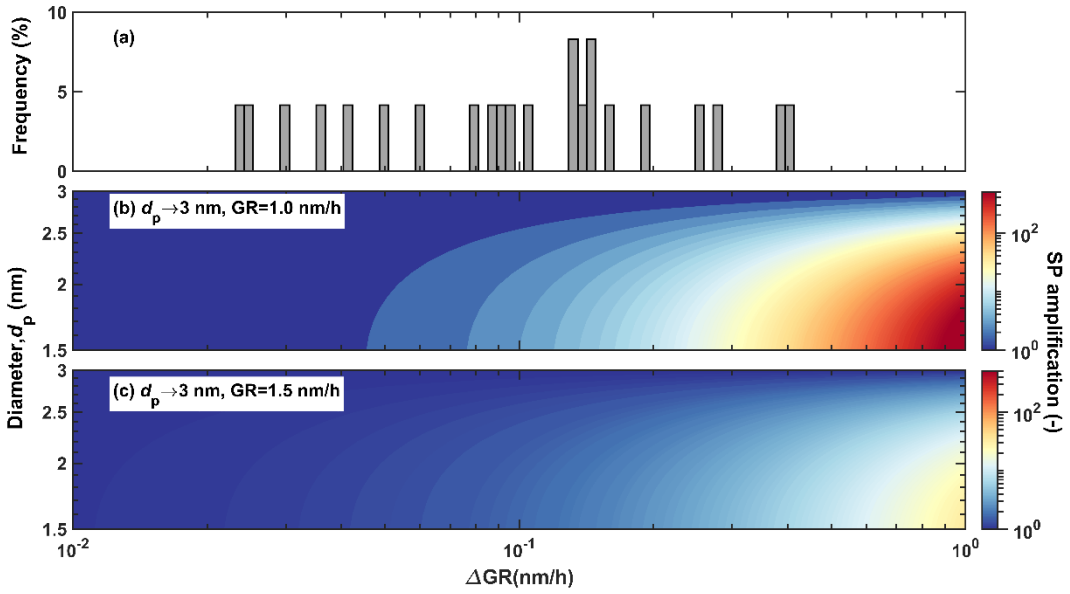

Figure S9: Amplification of survival probability under different GR enhancements and initial diameters. The amplification of SP is defined as the ratio of SP calculated with and without additional GR. (a)The frequency distribution of GR contribution of IA to sub-3 nm particle growth at the SORPES. (b) The amplification factor distribution of particles growing up to 3 nm with initial GR equals to 1.0 nm/h. (c) The amplification factor distribution of particles growing up to 3 nm with initial GR equals to 1.5 nm/h.

Tables

Table S1. NPF frequencies at both sites.

DATE	Beijing				Nanjing			
	NPFs	non-NPFs	valid days	frequency	NPFs	non-NPFs	valid days	frequency
2019-01	8	13	21	38.1%	-*	-	-	-
2019-02	8	20	28	28.6%	-	-	-	-
2019-03	14	15	29	48.3%	20	11	31	64.5%
2019-04	12	17	29	41.4%	12	18	30	40.0%
2019-05	12	17	29	41.4%	22	9	31	71.0%
2019-06	5	19	24	20.8%	16	14	30	53.3%
2019-07	4	26	30	13.3%	17	12	29	58.6%
2019-08	11	20	31	35.5%	21	10	31	67.7%
2019-09	9	21	30	30.0%	4	6	10	40.0%
2019-10	8	19	27	29.6%	11	3	14	78.6%

DATE	Beijing				Nanjing			
	NPFs	non-NPFs	valid days	frequency	NPFs	non-NPFs	valid days	frequency
2019-11	3	16	19	15.8%	12	13	25	48.0%
2019-12	9	19	28	32.1%	8	17	25	32.0%
2020-01	5	13	18	27.8%	7	23	30	23.3%
2020-02	5	20	25	20.0%	10	19	29	34.5%
2020-03	13	18	31	41.9%	-	-	-	-
2020-04	12	16	28	42.9%	-	-	-	-
2020-05	9	17	26	34.6%	-	-	-	-
2020-06	6	23	29	20.7%	-	-	-	-
2020-07	0	26	26	0.0%	-	-	-	-
2020-08	1	12	13	7.7%	-	-	-	-
2020-09	7	10	17	41.2%	-	-	-	-
2020-10	12	17	29	41.4%	-	-	-	-
2020-11	8	19	27	29.6%	-	-	-	-
2020-12	7	15	22	31.8%	-	-	-	-
2021-01	7	16	23	30.4%	-	-	-	-
2021-02	6	13	19	31.6%	-	-	-	-
2021-03	10	17	27	37.0%	-	-	-	-
2021-04	6	19	25	24.0%	-	-	-	-
2021-05	11	17	28	39.3%	-	-	-	-
2021-06	6	19	25	24.0%	-	-	-	-
2021-07	0	24	24	0.0%	-	-	-	-
2021-08	4	20	24	16.7%	-	-	-	-
2021-09	2	22	24	8.3%	-	-	-	-
2021-10	9	14	23	39.1%				
Total	249	609	858	29.0%	160	155	315	50.8%

Note: * represents the missing data.

Table S2. The GR contributions and SP enhancements of HIO_3 to particles in the size range between 1.5 nm to 3 nm on each NPF event days in Beijing based on APT-x.

Date	$CoagS_{1.5}$	$GR_{<3}$	GR_{H2SO4}	P1*	$GR_{<3}$ - GR_{HIO3}	P2*	GR contribution	$SP_{1.5-3}$ EF
20190818	2.21E-03	1.11	1.38	2.64E-03	1.07	2.16E-03	3.3%	22.2%
20190823	3.13E-03	3.01	1.63	4.57E-02	2.99	4.49E-02	0.5%	1.7%
20190830	1.91E-03	6.22	1.26	4.01E-01	6.17	3.99E-01	0.7%	0.7%
20210525	1.40E-03	2.98	0.66	2.49E-01	2.94	2.45E-01	1.2%	1.8%
20210526	3.58E-03	3.17	1.30	3.51E-02	3.08	3.20E-02	2.7%	9.8%
20210529	1.00E-03	0.68	0.54	1.26E-02	0.60	6.75E-03	12.5%	86.5%
20210619	1.30E-03	7.10	1.06	5.80E-01	7.05	5.78E-01	0.6%	0.3%
20210620	1.64E-03	3.92	1.11	2.90E-01	3.85	2.84E-01	1.9%	2.4%
20210621	4.81E-03	1.50	2.33	7.33E-05	1.33	2.18E-05	11.3%	236.2%
20210802	1.01E-03	2.11	1.02	2.41E-01	1.73	1.77E-01	17.9%	36.2%
20210827	2.51E-03	0.86	2.25	1.69E-04	0.55	1.40E-06	35.5%	11921.9%
20210929	2.43E-03	1.84	1.09	1.98E-02	1.79	1.77E-02	2.7%	11.8%

Note: P1 represents the survival probability calculated from measured GR; P2 represents the survival probability calculated from measured GR subtracted by GR contributed from HIO_3 concentration solely. Meanings of P1 and P2 in following Tables (Table S3~S7) are identical with them in this table.

Table S3. The GR contributions and SP enhancements of HIO_3 to particles in the size range between 1.5 nm to 3 nm on each NPF event days in Beijing based on APT-y.

Date	$CoagS_{1.5}$	$GR_{1.5-3}$	GR_{H2SO4}	P1	$GR_{1.5-3}$ - GR_{HIO3}	P2	$GR_{1.5-3}$ contributions	$SP_{1.5-3}$ EF
20190818	2.21E-03	1.80	1.38	2.61E-02	1.76	2.42E-02	2.0%	7.8%
20190823	3.13E-03	4.66	1.63	1.36E-01	4.64	1.35E-01	0.4%	0.7%
20190830	1.91E-03	8.40	1.26	5.09E-01	8.36	5.07E-01	0.5%	0.4%
20210525	1.40E-03	3.30	0.66	2.85E-01	3.26	2.81E-01	1.1%	1.4%
20210526	3.58E-03	5.13	1.30	1.26E-01	5.04	1.22E-01	1.7%	3.6%
20210529	1.00E-03	0.70	0.54	1.45E-02	0.62	8.08E-03	12.0%	78.9%
20210619	1.30E-03	8.38	1.06	6.30E-01	8.33	6.29E-01	0.5%	0.2%
20210620	1.64E-03	4.64	1.11	3.51E-01	4.56	3.46E-01	1.6%	1.7%
20210621	4.81E-03	1.92	2.33	6.07E-04	1.76	2.97E-04	8.8%	104.1%
20210802	1.01E-03	4.30	1.02	4.98E-01	3.92	4.65E-01	8.8%	6.9%
20210827	2.51E-03	1.11	2.25	1.23E-03	0.81	9.85E-05	27.4%	1151.9%
20210929	2.43E-03	2.87	1.09	8.12E-02	2.82	7.76E-02	1.8%	4.7%

Table S4. The GR contributions and SP enhancements of HIO_3 to particles in the size range between 1.5 nm to 3 nm on each NPF event days in Beijing based on MOD.

Date	$CoagS_{1.5}$	$GR_{1.5-3}$	GR_{H2SO4}	P1	$GR_{1.5-3}$ - GR_{HIO3}	P2	$GR_{1.5-3}$ contributions	$SP_{1.5-3}$ EF
20190830	1.91E-03	3.64	1.26	2.10E-01	3.59	2.06E-01	1.2%	2.0%
20210525	1.40E-03	0.84	0.66	7.30E-03	0.80	5.83E-03	4.4%	25.2%
20210526	3.58E-03	2.22	1.30	8.45E-03	2.14	6.98E-03	3.9%	21.1%
20210529	1.00E-03	0.90	0.54	3.73E-02	0.82	2.65E-02	9.4%	40.5%
20210619	1.30E-03	1.50	1.06	7.64E-02	1.46	7.10E-02	2.8%	7.7%
20210620	1.64E-03	1.00	1.11	7.78E-03	0.93	5.29E-03	7.4%	47.1%
20210621	4.81E-03	1.93	2.33	6.14E-04	1.76	3.01E-04	8.8%	103.7%
20210802	1.01E-03	1.40	1.02	1.18E-01	1.03	5.40E-02	26.8%	118.8%
20210827	2.51E-03	2.20	2.25	3.40E-02	1.90	1.97E-02	13.8%	72.1%

Table S5. The GR contributions and SP enhancements of HIO_3 to particles in the size range between 3 nm to 7 nm on each NPF event days in Beijing based on APT-x.

Date	$CoagS_3$	GR_{3-7}	P1	GR_{3-7} - GR_{HIO3}	P2	GR_{3-7} contributions	SP_{3-7} EF
20190818	7.40E-04	2.62	0.142	2.58	0.138	1.4%	2.8%
20190823	8.50E-04	5.83	0.365	5.79	0.363	0.6%	0.6%
20190828	2.39E-04	5.54	0.743	5.45	0.739	1.6%	0.5%
20190830	5.42E-04	5.87	0.529	5.82	0.526	1.0%	0.6%
20190914	7.19E-04	2.34	0.121	2.27	0.112	3.2%	7.3%
20190918	2.96E-04	2.15	0.387	2.11	0.380	1.7%	1.6%
20190924	5.89E-04	7.64	0.587	7.60	0.585	0.6%	0.3%
20200524	3.56E-04	3.61	0.506	3.39	0.485	5.9%	4.4%
20200526	2.92E-04	4.79	0.656	4.68	0.650	2.3%	1.0%
20200527	3.17E-04	15.24	0.866	15.03	0.864	1.4%	0.2%
20200614	1.48E-04	2.03	0.606	1.93	0.589	5.2%	2.8%
20200902	1.27E-03	2.96	0.051	2.89	0.048	2.3%	7.3%
20200903	1.62E-05	9.97	0.989	9.87	0.989	1.0%	0.1%
20210525	3.87E-04	4.60	0.559	4.57	0.557	0.7%	0.4%
20210526	9.44E-04	10.91	0.550	10.82	0.548	0.9%	0.5%
20210529	3.50E-04	0.55	0.013	0.46	0.006	16.3%	133.6%
20210619	3.90E-04	5.14	0.592	5.09	0.589	1.0%	0.5%
20210620	5.04E-04	7.42	0.626	7.36	0.623	0.8%	0.4%
20210621	1.35E-03	3.68	0.080	3.50	0.070	5.1%	14.6%
20210622	9.37E-04	5.82	0.329	5.66	0.319	2.8%	3.2%
20210802	3.30E-04	5.00	0.634	4.74	0.618	5.4%	2.6%
20210827	7.29E-04	4.57	0.332	4.29	0.309	6.2%	7.5%
20210929	6.02E-04	10.17	0.665	10.11	0.663	0.6%	0.3%

Table S6. The GR contributions and SP enhancements of HIO_3 to particles in the size range between 3 nm to 7 nm on each NPF event days in Beijing based on APT-y.

Date	$CoagS_3$	GR_{3-7}	P1	GR_{3-7} - GR_{HIO3}	P2	GR_{3-7} contributions	SP_{3-7} EF
20190818	7.40E-04	2.66	0.147	2.63	0.143	1.4%	2.7%
20190823	8.50E-04	5.87	0.368	5.84	0.366	0.6%	0.6%
20190828	2.39E-04	5.68	0.748	5.59	0.745	1.6%	0.5%
20190830	5.42E-04	5.91	0.531	5.85	0.527	1.0%	0.6%
20190914	7.19E-04	3.41	0.233	3.33	0.226	2.2%	3.4%
20190918	2.96E-04	2.18	0.392	2.15	0.386	1.7%	1.6%
20190924	5.89E-04	8.69	0.626	8.65	0.625	0.5%	0.2%
20200524	3.56E-04	3.81	0.525	3.60	0.505	5.6%	3.9%
20200526	2.92E-04	4.97	0.666	4.86	0.660	2.2%	0.9%
20200527	3.17E-04	16.19	0.874	15.98	0.872	1.3%	0.2%
20200614	1.48E-04	2.06	0.609	1.95	0.593	5.2%	2.8%
20200902	1.27E-03	3.27	0.068	3.20	0.064	2.1%	6.0%
20200903	1.62E-05	13.44	0.992	13.35	0.992	0.7%	0.1%
20210525	3.87E-04	5.75	0.628	5.72	0.627	0.6%	0.3%
20210526	9.44E-04	14.11	0.630	14.02	0.628	0.7%	0.3%
20210529	3.50E-04	0.89	0.066	0.80	0.049	10.2%	36.1%
20210619	3.90E-04	5.19	0.595	5.14	0.592	1.0%	0.5%
20210620	5.04E-04	7.45	0.627	7.39	0.625	0.8%	0.4%
20210621	1.35E-03	3.78	0.085	3.59	0.075	5.0%	13.8%
20210622	9.37E-04	5.98	0.339	5.82	0.329	2.7%	3.0%
20210802	3.30E-04	5.13	0.642	4.86	0.626	5.2%	2.5%
20210827	7.29E-04	4.86	0.355	4.57	0.333	5.8%	6.6%
20210929	6.02E-04	11.06	0.687	11.00	0.685	0.6%	0.2%

Table S7. The GR contributions and SP enhancements of HIO_3 to particles in the size range between 3 nm to 7 nm on each NPF event days in Beijing based on MOD.

Date	$CoagS_3$	GR_{3-7}	P1	GR_{3-7} - GR_{HIO3}	P2	GR_{3-7} contributions	SP_{3-7} EF
20190818	7.40E-04	2.75	0.156	2.71	0.152	1.3%	2.5%
20190823	8.50E-04	3.55	0.192	3.52	0.189	1.0%	1.6%
20190828	2.39E-04	3.56	0.630	3.47	0.622	2.5%	1.2%
20190830	5.42E-04	3.49	0.342	3.43	0.336	1.6%	1.8%
20190914	7.19E-04	2.99	0.190	2.91	0.182	2.5%	4.4%
20190918	2.96E-04	4.51	0.636	4.47	0.633	0.8%	0.4%
20190924	5.89E-04	3.13	0.273	3.09	0.268	1.3%	1.8%
20200524	3.56E-04	2.41	0.361	2.20	0.327	8.9%	10.4%
20200526	2.92E-04	2.95	0.505	2.84	0.491	3.7%	2.7%
20200527	3.17E-04	1.13	0.145	0.92	0.092	19.1%	57.6%
20200614	1.48E-04	2.46	0.660	2.35	0.648	4.3%	1.9%
20200902	1.27E-03	3.48	0.080	3.41	0.076	2.0%	5.2%
20200903	1.62E-05	4.32	0.974	4.22	0.974	2.3%	0.1%
20210525	3.87E-04	1.69	0.205	1.66	0.199	1.9%	3.1%
20210526	9.44E-04	4.43	0.229	4.33	0.222	2.1%	3.2%
20210529	3.50E-04	2.06	0.310	1.97	0.294	4.4%	5.5%
20210619	3.90E-04	3.90	0.501	3.84	0.496	1.3%	0.9%
20210620	5.04E-04	1.83	0.149	1.77	0.140	3.1%	6.2%
20210621	1.35E-03	1.93	0.008	1.74	0.005	9.7%	68.5%
20210622	9.37E-04	2.54	0.078	2.38	0.066	6.3%	18.7%
20210802	3.30E-04	1.82	0.286	1.55	0.230	14.8%	24.3%
20210827	7.29E-04	2.20	0.102	1.92	0.073	12.8%	39.9%
20210929	6.02E-04	1.89	0.111	1.83	0.103	3.3%	7.8%

Table S8. NPF event day identified at SOREPS and the contribution to growth of two acids in different size ranges and the ratio in each case.

DATE	$GR_{1.5-3}$(IA)	$GR_{1.5-3}$(SA)	$Ratio_{1.5-3}$
2019-06-17	0.15	2.39	6.1%

DATE	$GR_{1.5\text{-}3}$(IA)	$GR_{1.5\text{-}3}$(SA)	$Ratio_{1.5\text{-}3}$
2019-06-21	0.15	2.14	6.8%
2019-07-03	0.39	2.65	14.6%
2019-07-11	0.26	2.97	8.6%
2019-07-13	0.16	2.06	7.5%
2019-07-19	0.13	1.33	10.0%
2019-07-30	0.09	2.83	3.3%
2019-08-09	0.05	3.50	1.4%
2019-08-16	0.19	2.45	7.9%
2019-08-17	0.09	2.93	3.2%
2019-08-18	0.40	2.80	14.5%
2019-08-27	0.13	1.05	12.8%
2019-10-21	0.09	1.02	8.4%
2019-10-23	0.28	2.19	12.6%
2019-10-26	0.14	1.28	10.7%
2019-10-31	0.04	2.01	2.1%
2019-11-01	0.11	2.75	3.9%
2019-11-05	0.06	2.06	2.9%
2019-11-10	0.04	0.91	4.0%
2019-11-11	0.03	1.26	2.4%
2019-11-14	0.03	0.89	2.8%
2019-11-19	0.02	1.01	2.4%
2019-11-20	0.08	1.64	4.8%

Table S9. NPF event day identified at SOREPS and the contribution to particle survival probability of two acids in different size ranges and the enhancement of survival probability in each case.

DATE	$P_{1.5\text{-}3}$(SA)	$P_{1.5\text{-}3}$(SA+IA)	$E_{1.5\text{-}3}$
2019-06-17	-	-	-
2019-06-21	1.13E-03	1.75E-03	54.3%
2019-07-03	4.16E-03	8.34E-03	100.7%
2019-07-11	7.26E-03	1.07E-02	47.6%
2019-07-13	2.16E-03	3.32E-03	53.8%
2019-07-19	1.40E-02	2.07E-02	47.5%
2019-07-30	9.56E-03	1.11E-02	15.9%
2019-08-09	8.80E-02	9.10E-02	3.4%
2019-08-16	3.15E-03	4.80E-03	52.7%
2019-08-17	5.84E-04	7.37E-04	26.3%
2019-08-18	2.27E-02	3.66E-02	61.4%
2019-08-27	3.24E-03	6.20E-03	97.7%
2019-10-21	-	-	-
2019-10-23	-	-	-
2019-10-26	6.06E-04	1.24E-03	104.9%
2019-10-31	1.10E-05	1.39E-05	25.8%

DATE	$P_{1.5\text{-}3}$(SA)	$P_{1.5\text{-}3}$(SA+IA)	$E_{1.5\text{-}3}$
2019-11-01	9.15E-03	1.09E-02	19.1%
2019-11-05	1.32E-04	1.70E-04	29.1%
2019-11-10	-	-	-
2019-11-11	-	-	-
2019-11-14	-	-	-
2019-11-19	-	-	-
2019-11-20	-	-	-

References:

Cohen, M. D., Stunder, B. J. B., Rolph, G. D., Draxler, R. R., Stein, A. F., and Ngan, F.: NOAA's HYSPLIT Atmospheric Transport and Dispersion Modeling System, Bulletin of the American Meteorological Society, 96, 2059-2077, 10.1175/bams-d-14-00110.1, 2015.

Kulmala, M., Kerminen, V. M., Petäjä, T., Ding, A. J., and Wang, L.: Atmospheric gas-to-particle conversion: why NPF events are observed in megacities?, Faraday Discuss, 200, 271-288, 10.1039/c6fd00257a, 2017.

Manninen, H. E., Mirme, S., Mirme, A., Petäjä, T., and Kulmala, M.: How to reliably detect molecular clusters and nucleation mode particles with Neutral cluster and Air Ion Spectrometer (NAIS), Atmos. Meas. Tech., 9, 3577-3605, 10.5194/amt-9-3577-2016, 2016.

Wang, Y. Q.: MeteoInfo: GIS software for meteorological data visualization and analysis, Meteorological Applications, 21, 360-368, 10.1002/met.1345, 2014.